

# Does M31 result from an ancient major merger?

F. Hammer<sup>1</sup>, Y. B. Yang<sup>2</sup>, J. L. Wang<sup>1,2</sup>, M. Puech<sup>1</sup>, H. Flores<sup>1</sup> & S. Fouquet<sup>1</sup>  
*Laboratoire GEPI, Observatoire de Paris, CNRS-UMR8111, Univ. Paris-Diderot 5 place Jules Janssen,  
 92195 Meudon France*  
 francois.hammer@obspm.fr

## ABSTRACT

The M31 haunted halo is likely associated to a rich merger history, currently assumed to be caused by multiple minor mergers. Here we use the GADGET2 simulation code to test whether M31 could have experienced a major merger in its past history. It results that a  $3\pm0.5:1$  gaseous rich merger with  $r_{\text{pericenter}}=25\pm5$  kpc and a polar orbit can explain many properties of M31 and of its halo. The interaction and the fusion may have begun  $8.75\pm0.35$  Gyr and  $5.5\pm0.5$  Gyr ago, respectively. Observed fractions of bulge, thin and thick disks can be retrieved for a star formation history that is almost quiescent before the fusion. This also reports well the observed relative fractions of intermediate age and old stars in both the thick disk and the Giant Stream. In this model, the Giant Stream is caused by returning stars from a tidal tail which contains material previously stripped from the satellite prior to the fusion. These returning stars are trapped into elliptical orbits or loops for long periods of time which can reach a Hubble time, and are belonging to a plane that is 45 degrees offset from the M31 disk PA. Because these streams of stars are permanently fed by new infalling stars with high energy from the tidal tail, we predict large loops which scale rather well with the features recently discovered in the M31 outskirts.

We demonstrate that a single merger could explain first-order (intensity and size), morphological and kinematical properties of the disk, thick disk, bulge and streams in the halo of M31, as well as the observed distribution of stellar ages, and perhaps metallicities. It challenges the current scenarios assuming that each feature in the disk (the 10 kpc ring) or in its outskirts (thick disk, the Giant Stream and the numerous streams) are associated to an equivalent number of minor mergers. Given the large number of parameters, further constraints are certainly required to render better the complexity of M31 and of the substructures within its halo which ultimately may set up a more precise geometry of the encounter. This would allow, in principle, to evaluate the impact of such a major event to the Andromeda system and to the Local Group.

*Subject headings:* Galaxies: formation – Galaxies: halos – Galaxies: individual: M31 – Galaxies: interactions – (Galaxies:) Local Group – Galaxies: spiral

## 1. Introduction

Our nearest giant neighbour, M31 has attracted a considerable interest since the discovery of many large scale structures that surrounds its outskirts.

<sup>1</sup>Laboratoire GEPI, Observatoire de Paris, CNRS-UMR8111, Univ. Paris-Diderot, 5 place Jules Janssen, 92195 Meudon France

<sup>2</sup>NAOC, Chinese Academy of Sciences, A20 Datun Road, 100012 Beijing, China

These prominent structures include the Giant Stream (infall of  $1.5 \times 10^8 M_{\odot}$  stellar mass, Ibata et al. 2001) and the gigantic thick disk containing about 10% of the disk luminosity (Ibata et al. 2005). The halo of M31 is haunted by not less than 16 substructures that let Tanaka et al. (2010) conjecture that they are due to as many accretion events involving dwarf satellites with mass  $10^7$ - $10^9 M_{\odot}$  since  $z \sim 1$ . Observations at radio wavelengths (Westmeier et al. (2005); Thilker et al. (2004);

and references therein) reveal high velocity clouds, whose location and kinematics partly follow the Giant Stream. Moreover, a 10kpc, pseudo-ring inserted in the M31 disk dominates star formation (Baade & Arp 1964), HI gas (Roberts 1966), molecular gas (Nieten et al. 2006), and dust emission (Gordon et al. 2006).

Simulations of the numerous structures in the M31 outskirts have always assumed them to be caused by minor satellites. M32 is understood to be the perturber of the spiral arms (Byrd 1978, 1983), while NGC 205 has been modelled as the cause of the warp seen in the optical and HI disks of M31 (Sato & Sawa 1986). The thick disk has been modelled by earlier disruption, several Gyr ago, of dwarf galaxies on prograde orbits that are coplanar with the disk (Penarrubia et al. 2006). Simulations of the Giant Stream assumed a collision with an unknown satellite  $\sim 0.7$  Gyr ago (Font et al. 2006; Fardal et al. 2008). The 10 kpc ring could be also reproduced by an interaction with M32, assuming a polar orbit (Block et al. 2006).

In spite of their success to reproduce M31 structures, several of these simulations may be speculative because the M31 satellite orbits are currently unknown (e.g., Fardal et al. 2009). More problematic is the fact that stars in the Giant Stream (Brown et al. 2007) have ages from 5.5 to 13 Gyr, which is difficult to reconcile with a recent collision (e.g., Font et al. 2008). If the substructures are formed from different progenitors, why do they show obvious similarities in metallicity (e.g., Ferguson et al. 2005)? The main motivation for only investigating minor mergers is to preserve the M31 disk (Mori & Rich 2008). Indeed the M31 disk is not necessarily very old and permanent, as its associated stellar clusters display young to moderate ages ( $< 5$ -7 Gyr, Beasley et al. 2004), and most of stars in the outskirt structures are older than this. One should not discard that the gigantic structures may have been formed at the same time or even earlier than the disk. In fact many co-workers in the field (Rich 2004; Ibata et al. 2004; Brown et al. 2006) have hypothesised a possible major merger in the past history of M31<sup>1</sup>.

<sup>1</sup>Quoting van den Bergh (2005): “both the high metallicity of the M31 halo, and the  $r^{1/4}$  luminosity profile of the Andromeda galaxy, suggest that this object might have formed from the early merger and subsequent violent relaxation,

More recently, the kinematics of the M31 globular system has been attributed to an ancient major merger (e.g., Bekki 2010).

Understanding the nature of M31 has certainly an impact in cosmology because together with the Milky Way, they are the only two giant spirals in our immediate neighbourhood. Conversely to the Milky Way, M31 has properties (absolute K luminosity, angular momentum,  $[\text{Fe}/\text{H}]$  in the outskirts) similar to the average of large spirals having the same rotation velocity (Hammer et al. 2007). Half of the progenitors of spiral galaxies in this range were not relaxed 6 billion years ago, according to the detailed studies of their morphologies (Hammer et al. 2005; Neichel et al. 2008; Delgado-Serrano et al. 2010) and kinematics (Puech et al. 2008; Yang et al. 2008). Hammer et al. (2009) verified that various merger phases can reproduce quite well the observed morphologies and kinematics of these non-relaxed galaxies. This agrees with the disk rebuilding scenario (Hammer et al. 2005), according to which most spiral disks have been rebuilt following a major, gas-rich merger during the past 8-9 Gyr. High gas fractions have been shown to be essential during this process (Hopkins et al. 2008, 2010). Understanding the different substructures of M31 as resulting from a single event such as a gas-rich major merger is an important step to validate or dismiss such a channel for spiral disk formation.

The goal of this study is to investigate whether a past major merger, instead of multiple minor mergers, can reproduce most of the peculiarities of M31. The  $\Lambda$ CDM cosmology ( $H_0=70$  km s<sup>-1</sup> Mpc<sup>-1</sup>,  $\Omega_M = 0.3$  and  $\Omega_\Lambda = 0.7$ ) is adopted throughout the paper.

## 2. Observational constraints and initial conditions

We assume in the following that M31 results from a past major merger. Our goal is to simultaneously reproduce: (1) the M31 disk at its rotation velocity, and the bulge, with B/T=0.28; (2) the presence of a very extended, co-rotating thick disk; (3) the 10kpc dust, HI, star-forming ring; (4) the Giant Stream, and (5) the observed age distributions of stars in the different substructures.

of two (or more) relatively massive metal-rich ancestral objects.”

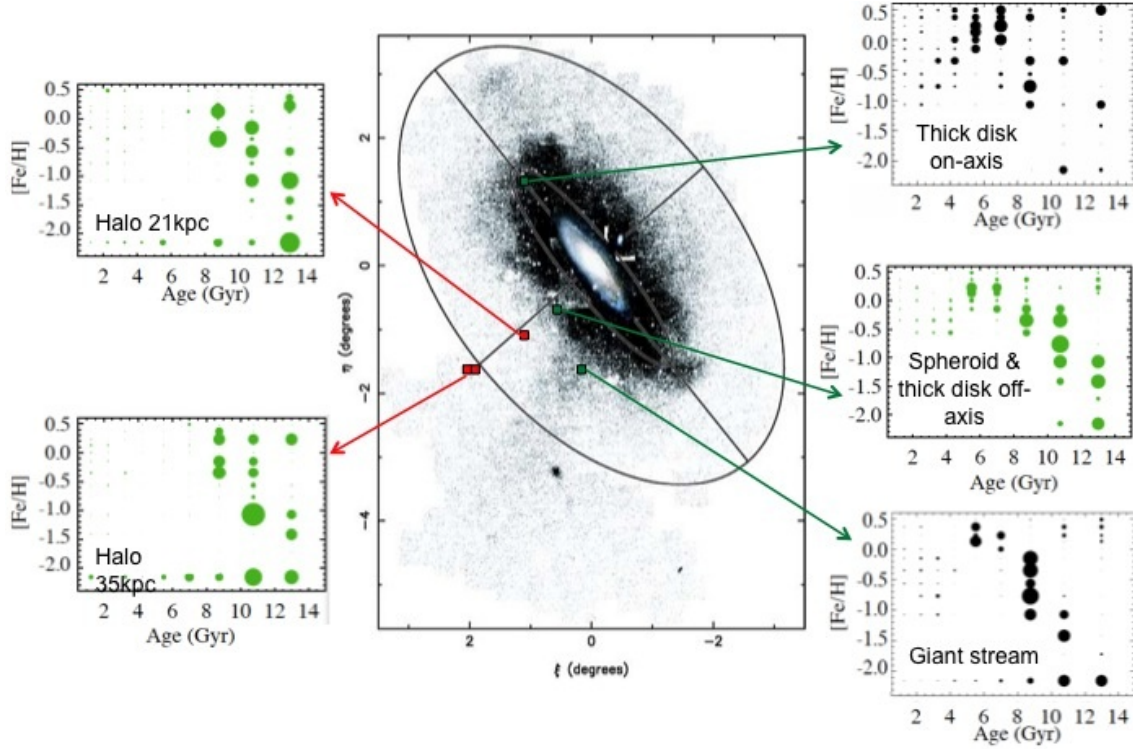


Fig. 1.— Chronological sketch of the structures surrounding M31. In the central panel (reproduced from Ibata et al. 2005), the large and thick rotating disk is a vast flattened structure with a major axis of about 4 degrees. Squares represent fields observed by Brown et al. (2006, 2007, 2008), and are related by arrows to their measurements.

Such a choice may appear somewhat subjective although it has been thoroughly adopted after reviewing many of the M31 properties. First, because the M31 system is very complex to model, we need to limit the number of features that can be reproduced. Second, the limitations of our model (number of particles) prevent us to describe very small structures, for example the double nucleus of M31 (but see Hopkins & Quataert 2010). Third we aim at reproducing the zero and first order features of each substructures of M31, including their stellar age, mass, and kinematics (if they are available from observations), but not the detailed morphology of each of them (see discussion, section 5).

According to Hopkins et al. (2010) (see their Figure 7), a mass ratio from 0.3 to 0.5 is required to reform a new bulge with  $B/T \sim 0.3$  in the rem-

nant galaxy for gas fractions<sup>2</sup> ranging between 0 and 50%. However, reforming a significant thin disk requires that enough gas is preserved after the fusion of the cores: it is mostly made of stars from the gaseous thin disk that immediately reforms after the collision (Barnes, J.E. 2002; Abadi et al. 2003; Governato et al. 2007; Hopkins et al. 2009). Thus reforming an Sb galaxy like M31 probably requires a gas fraction in excess of 50% in the progenitors. The total baryonic mass of M31 is  $1.1 \times 10^{11} M_{\odot}$  (Hammer et al. 2007), and at first approximation we can assume that this is the value for the sum of the two progenitor masses. In order to prevent a too violent relaxation in the center of the main progenitor, we adopt a prograde-retrograde orientation of the spin axes, which has been shown to be more favorable in rebuilding a

<sup>2</sup>the gas fraction in the progenitors should reach a higher value than in Hopkins et al. (2010), since they define the gas fraction as its value just before the fusion

thin disk after a major merger (Hopkins et al. 2008).

The presence of a gaseous ring favours a polar orbit. As shown by Mori & Rich (2008), the Giant Stream may result from the returning material of the tidal tail formed just before the last passage of the satellite. A similar although longer-lived tidal tail is predicted for a 3:1 major merger with polar orbit, which is associated to the passage of the secondary galaxy just before fusion. During the first passage and until the fusion, star formation is especially enhanced into the secondary galaxy that is harassed by the main one (e.g., Cox et al. 2008). If the Giant Stream was associated to returning particles from the tidal tail formed during the second passage (near fusion), it would contain mostly stars older than the epoch of the fusion: this is because the star formation cannot hold for a long time within tidal tails due to their expected dilution.

We thus propose from Fig. 1 a chronological history of the different structures in M31, as this Figure can be used as a clock for determining the occurrence of merger phases. The star formation history of the whole system is enhanced during the first passage until the fusion and then at the fusion itself (see Cox et al. 2008). During a merger event, most of the gas and stars in the remnant outskirts have been deposited by tidal tails formed during the first passage and later on, during the fusion of the cores. Few hundred billion years after its formation, the tidal tail dilutes, provoking a natural quenching of the residual star formation (see Wetzstein et al. 2007). Thus the age of the material brought by tidal tails provides, with a relatively small delay, the date of either the first passage and fusion times. In the following, we assume that the first passage occurred from 8.5 to 9 Gyr ago, and that the corresponding tidal tails are responsible for the halo enrichment seen in the 21 kpc and 35 kpc fields, without significant star formation more recent than 8.5 Gyr. The thick disk has a star formation history comparable to that of the Giant Stream, and is also generated by material returning to the galaxy mostly from tidal tails generated at the fusion. Because their youngest significant population of stars have ages of 5.5 Gyr, the delay between first passage and fusion ranges between 3 and 3.5 Gyr. This could be accommodated for by relatively large impact

parameters (20 to 30 kpc).

From the above, we can settle the initial conditions for a major merger assumed to be at the origin of M31. Table 1 describes the adopted physical parameters of such an interaction. Given the huge amount of observational data, it is beyond the scope of this study to reproduce the details of all the numerous structures in the M31 system. Instead, our use of hydrodynamic simulations is to determine whether or not these numerous substructures can be attributed to a single major merger in the past history of M31.

### 3. Simulations

We used the GADGET2 hydrodynamical code (Springel 2005) and initial conditions similar to that of Cox et al. (2006, 2008). For the dark matter, we adopted a core density profile as in Barnes, J.E. (2002), with a core size of 5.3 kpc and 3.06 kpc for the main galaxy and the satellite, respectively. We verified that our results are not significantly affected by changing the density profile to a Hernquist model that is quite similar in central regions to a NFW model (see section 5). Concerning the implementation of feedback and cooling, we have verified step by step our ability to reproduce both the isolated and merger cases for all the different combinations of feedback and cooling in Cox et al. (2008), and as such, all parameters used in our simulations are very similar to those of Cox et al. (see Wang 2010, in preparation). Usually, the free parameters describing the star formation efficiency and the feedback strength are chosen in order to match to Schmidt-Kennicutt law between star formation and gas surface densities (see Cox et al. 2006). Given the relatively large scatter of this relation, a large number of combinations can be accommodated (Cox et al. 2006, 2008). In the following, we explored several combinations that are in agreement with this relation, but with the additional constrain of preserving a significant gas reservoir in the progenitors, before fusion (see Sect. 4.2). Properties of the progenitors are listed in Table 1, and these galaxies have been generated to follow the baryonic Tully Fisher relation (see Puech et al. 2010, for an argument in favour of a non-evolving relation). Their atomic gas content has been assumed to be three times more extended than the stars, as also adopted by

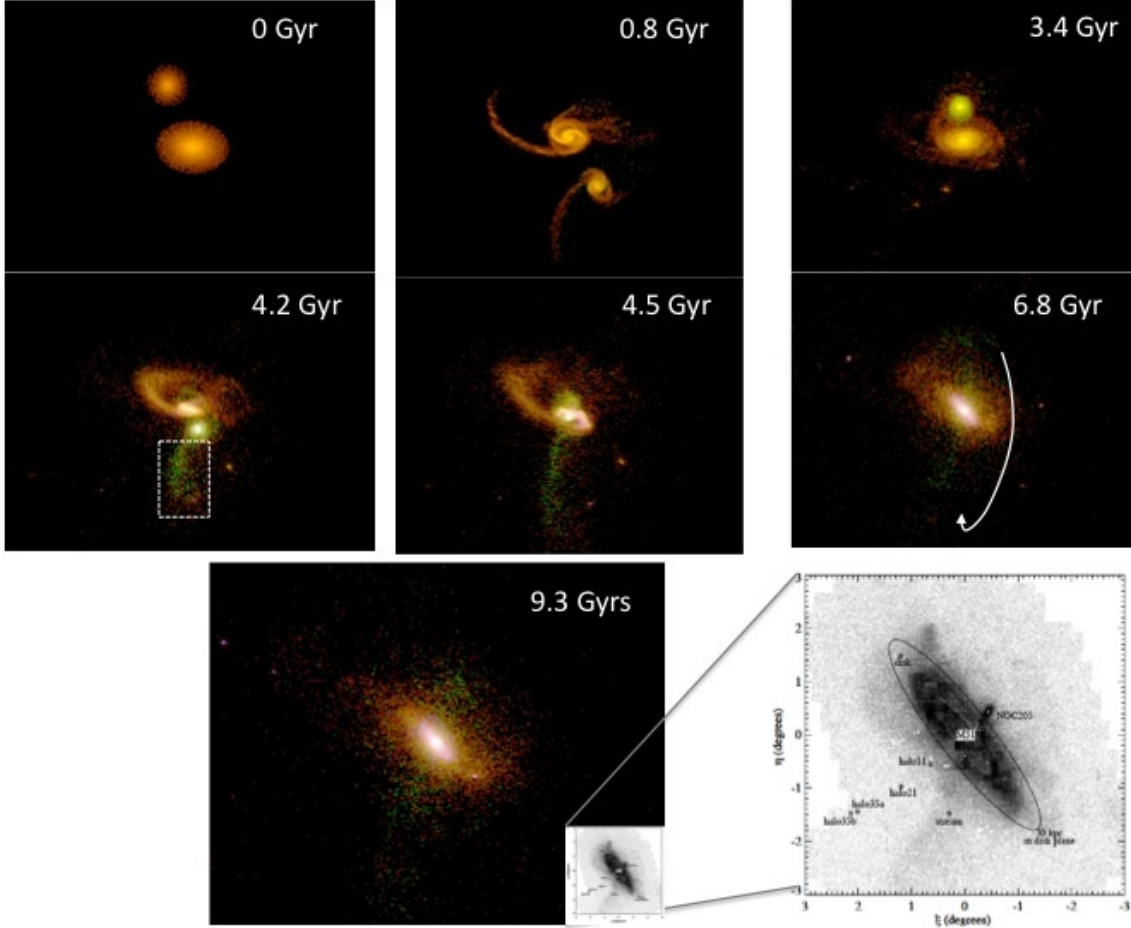


Fig. 2.— Different phases of a 3:1 major merger for M31 ( $r_{\text{pericenter}}=24$  kpc, Gal1  $\text{incy}=70$ , Gal2  $\text{incy}=-110$ ). The simulation starts 9.3 Gyr ago ( $T=0$ ,  $z=1.5$ ) and the first passage occurs 0.7 Gyr later. Then new stars are forming (color code: green), especially in the secondary galaxy, until the fusion, which occurs at 4.5 Gyr. The elapsed time between first passage and fusion is 3.8 Gyr, as the pericenter radius is large. During the second passage ( $T=4.2$  Gyr) a tidal tail containing many newly formed, intermediate-age stars (green dots) is formed. Later on this material returns to the galaxy forming the Giant Stream, enriched with stars formed from 5 to 8 Gyr ago. The resulting galaxy in the last panel ( $T=9.3$  Gyr) is compared with the inserted M31 image at the same scale (from Ibata et al. 2005, , see an enlarged view of this insert on bottom-right). The Figure illustrates also the formation of the Giant Stream (see section 4.4) in a case for which the two galaxies have angle difference near the resonance (180 degrees) providing many particles stripped from the satellite at 4.2 Gyr. Some of particles within the tidal tail have velocity below the escape velocity of the remnant system and are gradually falling back to the galaxy. They are tracing loops around the newly formed disk as indicated by the arrow in the panel at  $T=6.8$  Gyr. Loops are fed by newly particles falling back from the tidal tail and are persistent until 9.3 Gyr and later. The dotted rectangle in the 4.2 Gyr panel illustrates how we have selected the tidal tail particles (see section 4.4).

Table 1: Initial and adopted conditions for a major merger model for M31.

Ingredient	tested range	comments	adopted range
total mass	$5.5 \times 10^{11} M_{\odot}$	20% of baryons	-
mass ratio	2-4	to reform B/T $\sim$ 0.3	2.5-3.5
$f_{gas}$ Gal1	0.4-0.6	expected at $z=1.5^a$	0.6
$f_{gas}$ Gal2	0.6-0.8	expected at $z=1.5$	0.8
Orbit	near polar	to form the ring	-
Gal1 incy <sup>b</sup>	10 to 90	Giant Stream	35-75
Gal2 incy <sup>b</sup>	-30 to -110	Giant Stream	-55 to -110
Gal1 incz <sup>c</sup>	90 to 110	Giant Stream	90-110
Gal2 incz <sup>c</sup>	90 to 110	Giant Stream	90-110
Spin Gal1	prograde	-	-
Spin Gal2	retrograde	significant remnant disk <sup>d</sup>	-
$r_{pericenter}$	20-30 kpc	see text	22-30 kpc
Feedback	high-medium <sup>e</sup>	to preserve gas	high/varying <sup>e</sup>
$c_{star}$	0.004 <sup>f</sup> -0.03	to preserve gas	0.03

<sup>a</sup>Daddi et al. (2010) found  $f_{gas}=0.5-0.65$  in galaxies with  $M_{baryon}=0.8-2.2 \cdot 10^{11} M_{\odot}$  at  $z=1.5$

<sup>b</sup>Orientation of the angular momentum of Gal1 relative to the orbital angular momentum, y axis

<sup>c</sup>Orientation of the angular momentum of Gal1 relative to the orbital angular momentum, z axis

<sup>d</sup>Following Hopkins et al. (2008)

<sup>e</sup>In some simulations, the feedback is assumed to be high before fusion and later on, assumed to drop to the medium or low feedback values of Cox et al. (2008); see also section 4.2)

<sup>f</sup>Another way to preserve the gas before fusion for allowing a significant amount of gas in the disk

Cox et al. (2006); see also an observational support from van der Kruit (2007) and references therein). We have to preserve enough gas immediately after the fusion to preserve the formation of a significant thin disk with more than 50% of the baryonic mass.

During our investigations to optimise the orbital parameters, we run the GADGET2 code with 150000 particles. In most simulations, we have ensured that the mass of dark matter particles is no more than twice that of initial baryon particles, i.e. gas or stars in the progenitors. During star formation events controlled by the gas volume density (and following Kennicutt-Schmidt law), we have also limited the number of newly formed stars per gas particle to three. This is an important limitation to the simulation as we have verified that when newly borne stars are relatively too small in mass, they are artificially scattered due to their encountering with heavy dark matter particles. Similarly, we need to keep the mass of dark matter particles low enough to avoid non-

physical disruption of the newly reformed disk at the end of the simulation. In the following we have tested that the decomposition of the newly formed galaxy does not depend on the adopted number of particles within the range of 150 000-800 000.

However, simulating the first order properties of faint structures like the Giant Stream requires a high particle number: the Giant Stream is made of  $3 \cdot 10^8 M_{\odot}$ , which corresponds to 1/366th of the total baryonic mass of the galaxy, and lets only a few hundreds of particles in the Giant Stream for a 150 000 particles simulation. Having fixed the range of parameters to reproduce the observed decomposition of M31 in bulge, thin and thick disks, we used a limited number of simulations with 300 000 to 800 000 particles to better identify the formation of faint structures.

Table 1 lists the adopted range of parameters which have been investigated (2nd column) and adopted (column 4) for several models considered in this study. These models are all part of the same family of orbital parameters, and they differ essen-

tially by various adjustments of the the star formation history or small variations of orbital parameters. We have begun with a model with moderate gas fractions (40% and 60% in Gal1 and Gal2, respectively) to verify whether a significant thin disk can be formed after fusion, assuming somewhat extreme conditions (e.g., high feedback and very low star formation efficiency) to prevent star formation before the fusion epoch. We then realised that most of the gas preserved before fusion forms a very thin disk (see also Abadi et al. 2003), which also hosts some of the pre-existing stars before fusion. However, the thin disk fraction is generally not much larger than the available gas fraction before fusion. Because about 65% of M31 stars lie in the thin disk, we have generated for our current models a higher gas fraction that allows us to test less extreme conditions for feedback and star formation efficiency. Indeed, such gas fractions are quite common at  $z=1.4$  (see Daddi et al. 2010), a redshift which corresponds to 9 Gyr ago, just before the interaction between the M31 progenitors (see section 2). Finally the models adopted in Table 1 (column 4) are developed to optimise the reproduction of the decomposition of the galaxy in bulge, thin and thick disks, and the disk scale length (see sections 4.1 and 4.2), the presence of the 10 kpc ring (see section 4.3), the Giant Stream and its kinematics (see section 4.4), as well as the fraction of stellar ages in most of these substructures (see sections 4.2 and 4.4). An overview of the goodness of each model is provided in section 5.

Figure 2 shows the different steps of the merger for one of our models. At the first passage (at  $T=0.7$  Gyr), tidal tails are formed and enrich the halo, although they are mostly diluted at the fusion epoch. Part of the material ejected during the second passage and the fusion progressively return to the galaxy after the fusion. The material associated with the tidal tail pointing to the bottom of the galaxy (see panel at  $T=4.2$  Gyr) possesses an angular momentum very different from that of the newly formed disk. This perturbation may explain such faint features like the Giant Stream, and could be persistent for several Gyr after fusion (see section 4.4).

## 4. Results and comparison with observations

### 4.1. Decomposition of the newly formed galaxy in sub-components

We choose to decompose the newly formed galaxy in three components, according to the relative strength of the angular momentum in the direction of that of the thin disk, which is approximately the orbital angular momentum. A very accurate determination of the thin disk angular momentum is possible because most of the preserved gas particles before the fusion naturally form a thin disk (see also Abadi et al. 2003) in which most of the star formation occurs after fusion. We have used the stars born 0.5 Gyr after the fusion to determine the angular momentum of the newly formed disk (see Fig. 3). With this technique, we obtain an accuracy of  $\pm 1$  degree for determining both the disk PA and inclination.

Fig. 4 (top panels) shows the ratio of the angular momentum along the y axis to the total angular momentum ( $J_Y/J_{total}$ ) as a function of the x-axis along which the thin disk is projected (see Fig. 3). The final disk rotates anti-clockwise (see Chemin et al. 2009) and the thin disk (illustrated in Fig. 3) is easily recognisable in the Fig. 4 top-left panel for values ranging from -0.9 and -1, which corresponds to the gaseous thin disk. Other recently formed stars are located within a compact structure without preferred angular momentum orientations, which corresponds to the bulge. Ibata et al. (2007) pointed out the confusion in the literature between the spheroid component and the thick disk. They revealed that the minor-axis region between projected radii of  $7 \text{ kpc} < R < 18 \text{ kpc}$  is strongly affected by a rotationally-supported thick disk that correspond to approximately one tenth of the thin disk stellar mass<sup>3</sup>. For a better comparison with observational data, we assume that the thick disk is made by all particles (but those of the thin disk) whose angular momentum is dominated by rotational motions along the thin disk. It means that  $J_Y$  has to be larger than the combination of other components

<sup>3</sup>It is important to notice that this region (quoted as "spheroid and thick disk off-axis" in Fig. 1) could be well dominated by the spheroid (Tom Brown, private communication), depending on the precise density profiles of both spheroid and thick disk.



of the angular momentum (i.e.  $\sqrt{J_X^2 + J_Z^2}$ ), i.e.,  $J_Y/J_{total}$  should be larger than  $-1/\sqrt{2} = -0.707$ , as illustrated by the dot-dashed lines in Fig. 4. We have generated the decomposition proposed by Abadi et al. (2003) for comparison. In their scheme, the thick disk is the residue after subtracting the bulge and the thin disk assuming a bulge symmetrically distributed around  $J_Y=0$ . While the thin disk fraction is found to be very similar with both approaches, the residual thick disk from Abadi et al.'s method is almost twice than what is provided by our method. We notice that a significant fraction (up to 50%) of such a residual thick disk is made of particles which are not dominated by rotation around the Y-axis, which explains well the discrepancy. For comparison with the Ibata et al. (2005) observations of a rotationally-supported thick disk, we keep our decomposition as it is described above.

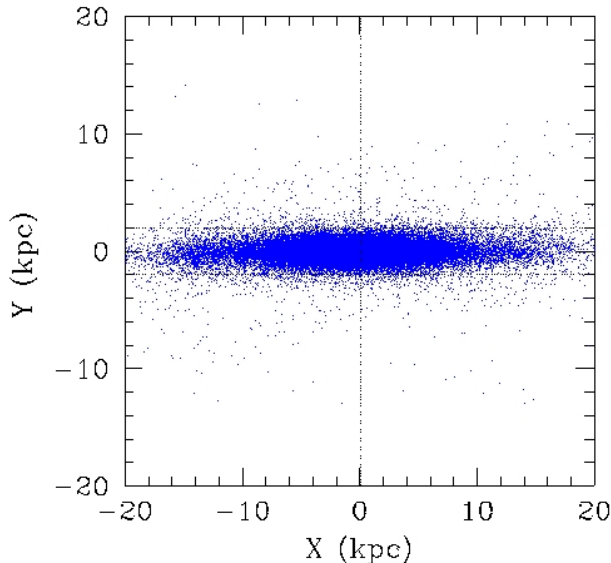


Fig. 3.— Distribution of newly formed stars 0.5 Gyr after the fusion which occurs 5 Gyr after the beginning of the simulation, for a 2.8:1 merger with  $r_{per}=30$  kpc, Gal1 incy=65 and Gal2 incy=-90. 10 Gyr after the simulation, the diameter of the newly formed disk reaches  $\sim 36$  kpc for a thickness of 4 kpc (see thin lines) in a model for which high feedback has been assumed during all the duration of the merger. Here the thin disk has been projected along the X-axis, and its angular momentum is oriented along the Y-axis.

Table 2: Decomposition in mass (unit= $10^{10} M_\odot$ ) of the newly formed galaxy 9 Gyr after the simulation, for various parameters of our modelling. For all models but the last one, high feedback has been maintained during all the simulation. For the last simulation, feedback has been abruptly dropped from high to low values (from Cox et al. 2008), 3.5 Gyr after the beginning of the simulation and  $\sim 0.7$  Gyr after the fusion.

Parameters	Comp.	Thin disk	Bulge	Thick disk
$r_{pericenter}=24$	Stars	2.66	2.51	0.85
mass ratio =3.5	Gas	3.24	0.15	0.09
Gal inc=65 & -110	Fraction	62%	28%	10%
$r_{pericenter}=24.8$	Stars	2.72	2.31	0.78
mass ratio =3.0	Gas	3.34	0.12	0.11
Gal inc=65 & -89	Fraction	65%	26%	9%
$r_{pericenter}=24.8$	Stars	2.38	2.67	0.95
mass ratio =2.8	Gas	2.95	0.13	0.10
Gal inc=65 & -89	Fraction	60%	29%	9%
$r_{pericenter}=24$	Stars	2.25	2.84	0.88
mass ratio =2.5	Gas	2.91	0.12	0.09
Gal inc=65 & -89	Fraction	57%	32%	10%
Same as above	Stars	3.62	2.61	1.22
feedback	Gas	1.32	0.07	0.12
changed at 3.5Gyr	Fraction	55%	29%	14%

#### 4.2. Thin and thick disks: feedback prescriptions

Table 2 describes how the decomposition depends on the choice of orbital parameters. From the 2nd to the 4th sets of parameters, only the mass ratio is varying and the bulge fraction increases as the mass ratio decreases as shown by Hopkins et al. (2009). However we have also tested a higher mass ratio (1st set of parameters) with a different set of inclinations for the progenitors. Thus the bulge fraction may also depend on other orbital parameters, here the relative inclination of the progenitors. For example it reaches a maximum when the difference of inclination between the two progenitors is close to 180 degrees, possibly because more stars take radial orbits and fall into the bulge. It will be shown later in section 4.4 that this resonance has a more considerable effect to the matter that is stripped from the satellite to



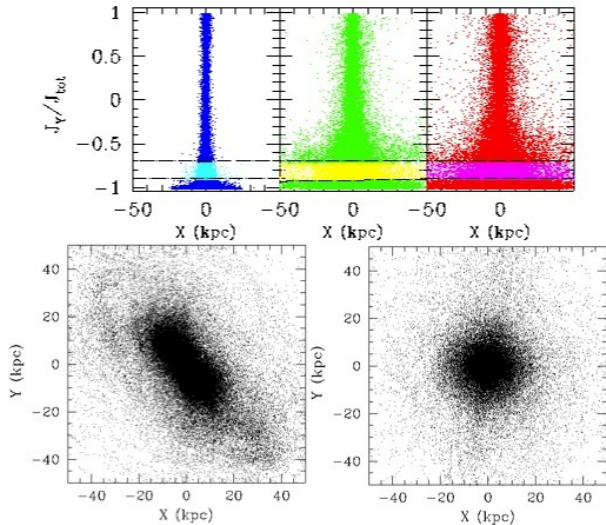


Fig. 4.— *Top*: adopted decomposition of the newly formed galaxy (same model as in Fig. 3), 10 Gyr after the simulation. Here the thin disk has been projected along the X-axis as in Fig. 3. Blue, green and red dots shown in the three panels represent stars formed 0.5 Gyr after the fusion, stars formed between the first passage (0.5 Gyr after the fusion, from the bottom to the top), stars formed between the first passage (0.5 Gyr after the fusion, from the bottom to the top), stars within the progenitors, respectively. The two dot-dashed lines delineates the thin and the thick disk, from the bottom to the top. *Bottom*: particles distribution in the thick disk (left panel) and in the bulge (right panel). Here the thick disk and the bulge have been projected at the right orientation of M31 thin disk (e.g. PA=38 degree and inclination=77 degrees).

the tidal tail at the 2nd passage.

Almost all the simulations we have generated are re-forming significant thin disks containing more than half of the baryonic mass. This is due to our feedback prescriptions that always preserve a significant fraction of gas just before the fusion. As quoted from Cox et al. (2008), very little is known about the requisite conditions enabling the star formation to occur. An important prerequisite however is to warrant the presence of stable gas rich galactic disks at high redshifts, as could be the progenitors of M31. Cox et al. (2008) have tested feedback for an isolated disk galaxy with an initial gas fraction of  $f_{gas}=0.52$ . They found that the gas fraction is mostly preserved within

one Gyr if median to high feedback prescriptions are adopted, while low feedback decreases the gas fraction to 0.37 in the same amount of time.

In our current models we have assumed  $f_{gas} \sim 0.65$ : the re-formation of a significant thin disk implies that most of the gas is not transformed into stars before fusion. This calls for relatively high feedback, at least intermediate between the median and high values of Cox et al. (2008). We have verified that for half the value of high feedback of Cox et al. (2008), most of the initial gas is preserved before the fusion. However, re-forming a significant stellar thin disk requires a significant change of the feedback at or after the fusion, in order to transform stars from the gas in the newly reformed disk. It results that from the merger of realistically gas-rich galaxies at  $z \sim 1.4$ , we may reform a galaxy resembling to M31, at the condition of a transitory history of the feedback during the merger, from high to low values. There could be some theoretical grounds favouring such an history, however. For example, in a gaseous rich and almost pristine medium, first supernovas are likely massive and generate high feedback as they may delay star formation for up to 100 Myr (e.g., Bromm et al. 2009). The fusion of two gaseous-rich galaxies corresponds to a severe mixing of most of their components, accompanied with large star formation rates. Then the metal abundance in the remnant becomes larger and more homogeneously distributed than it was in the progenitors, before fusion. The occurrence of very massive, primordial supernova is unlikely in such a mixed medium leading to a possible transition from high to low feedback. Before the fusion there is much less exchanges between the two interlopers, and it might be realistic to assume a negligible change of the feedback history.

Of course the above is mostly made of conjectures in absence of observations of gas-rich galaxies at high redshift showing no or very small amounts of star formation, i.e., the high-redshift counterparts of the present-day low surface brightness galaxies. We may however verify whether our adopted star formation history is consistent or not with the star formation history revealed in each M31 substructure displayed in Fig. 1. The thick disk is indeed mostly made by matter returning from the tidal tails. It comprises approximately 80% of stars older than 8 Gyr, the rest being

mostly stars from 5 to 8 Gyr. Such a distribution is well reproduced by our model with high feedback values (86% of old stars) or with half this value (80%). Because the thick disk shows a similar fraction of stars in the two bins set by Brown et al. (2008) at 5.5 and 7 Gyr, it is probable that there are no significant changes of the star formation history between the two corresponding epochs, i.e. between the first and second passage.

Within these prescriptions our models predict quite well the fraction of each sub-component of M31 (see Table 2). Notice also that the modelled thin disks show rotation curves and scalelengths that are in good agreement with observations (see Fig. 5). In the next sections we examine whether this model could also reproduce other large scales structures such as the ring and the Giant Stream.

#### 4.3. The 10 kpc ring

The decomposition of the light profile has been done by fitting the radial profile with a 3 components model (bulge, thin, thick disks). It provides a thin disk with a Sersic index of 1 and a scale-length varying from 4.8 to 5.1 kpc for models with mass ratio ranging from 3 to 2.8. Such values are slightly smaller than  $5.8 \pm 0.4$  kpc that was adopted by Hammer et al. (2007) for the M31 disk. All these decompositions (see Fig. 5) reveal the presence of a prominent ring at 10 kpc which corresponds well to the observed ring. Similarly all models reproduce the 10 kpc gaseous ring (see Fig. 6) as seen in HI observations. This is not unexpected as all the orbits are close to polar which favours the formation of such prominent and persistent structures. In fact, HI observations do not provide much constraints on our modelling. They only discard parameters for which the disk is too warped, i.e. implying that the difference between the two inclination angles of the progenitors should not be too close to 180 degrees. Moreover, we notice (see Fig. 6) that with a constant high feedback during the simulation, there are still gas within the bulge of the remnant galaxy. However this gas is consumed in models that assume a transition to low feedback immediately after the fusion.

#### 4.4. The Giant Stream and its kinematics

The Giant Stream is a very faint stellar structure, which extends from 50 to 80-100 kpc from

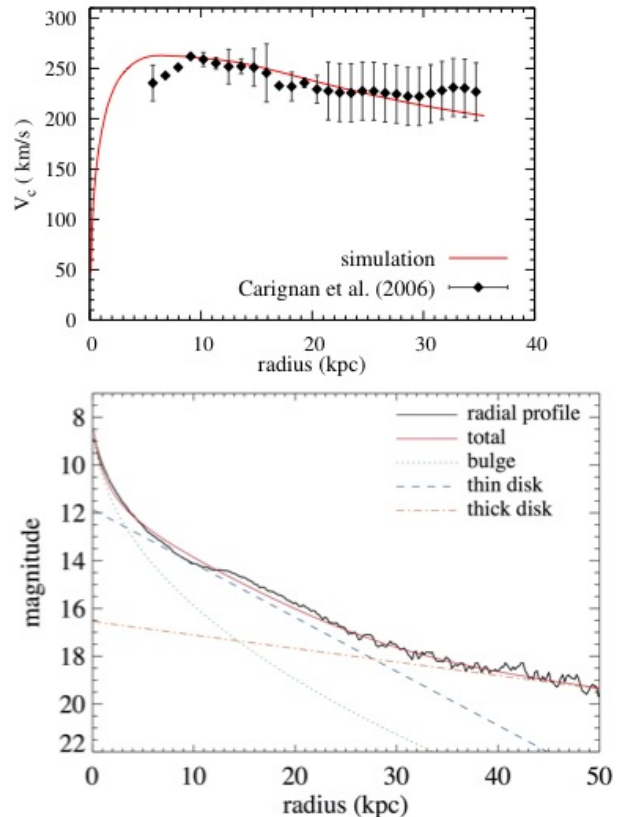


Fig. 5.— 3:1 merger with  $r_{\text{pericenter}}=24.8$  kpc, 9 Gyr after the beginning of the simulation. *Top*: Rotation curve of the thin disk compared to Carignan et al. (2006). There is a particularly good agreement between our modelling and data from Carignan et al. (2006). *Bottom*: Decomposition of the mass profile in 3 components which evidences the 10kpc ring and provide a thin disk scalelength of 5 kpc.

the M31 centre. We have modelled it as caused by particles coming back from the tidal tail formed just before fusion. Fig. 2 describes the formation of such a structure that is aligned along the trajectory of the satellite which falls into the mass centre at the fusion, 4.5 Gyr after the beginning of the simulation. We verified that, within the family of orbits we choose, the strength of the tidal tail (see Fig. 2, panel at 4.2 Gyr) depends on the inclination of the progenitors relatively to the orbital angular momentum (see Table 1). Optimal values are found for large values of the inclination of the main galaxy ( $> 50$  degrees) and especially

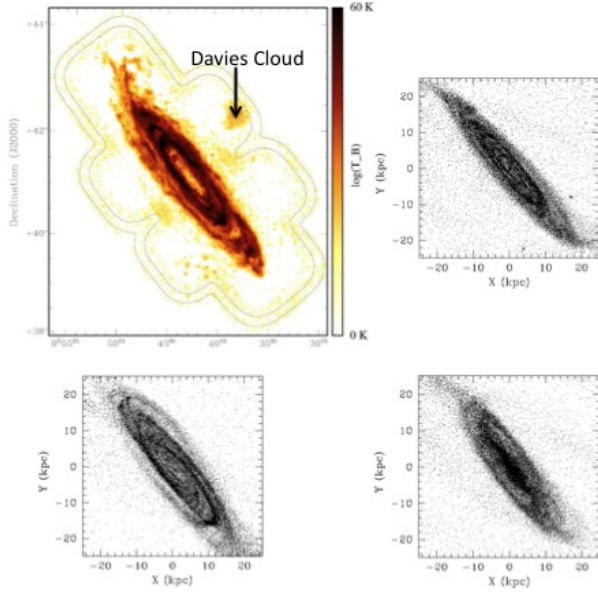


Fig. 6.— Comparison of the HI gas from Braun et al. (2009) with modelling of gas particles for 3:1 mergers at  $T=9$  Gyr. On the top-right and bottom-left models are with  $r_{per}=24.8$  kpc, and inc of 65 and -95 degrees for the main galaxy and the satellite. The two models have a feedback varying from high to low value near the fusion time, and they do not show gas excess in the central bulge. They only differ by a small variation of 5 degrees in their inclinations along the  $z$ -axis. On bottom-left is shown a model with a constant high feedback and with a difference between the two galaxies inclination of 170 degrees. It illustrates that changing feedback is necessary to explain the absence of gas in the centre and that inclinations should not be too close to 180 degrees to avoid too large distortions of the final gaseous disk.

for difference between the inclination of the two progenitors between 140 to 170 degrees, i.e. not too far from the resonance at 180 degree.

Modelling the Giant Stream is not an easy task as the structure is very faint compared to other large substructures of M31, even the thick disk. As in section 4.1 we make use of angular momentum properties to identify peculiar structures able to persist after the remnant phase (see Fig. 7).

Fig. 7 shows the distribution of the angular momentum for the thick disk (top-left panel) and at the galaxy outskirts, 5 Gyr after fusion. The top-

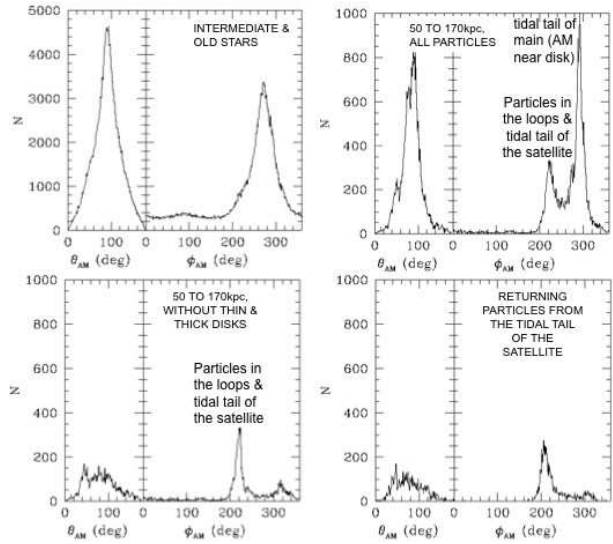


Fig. 7.— 2.8:1 merger with  $r_{pericenter}=30$  kpc. Distribution of the angular momentum 5 Gyr after fusion using spherical coordinates, assuming the thin disk perpendicular to the  $y$ -axis. *Top-left*: stars formed before fusion (intermediate and old stars) which show a broader distribution than thin disk stars as it is expected for the thick disk that hosts most of these stars (see Table 2). *Top-right*: angular momentum distribution for particles beyond 50 kpc from the centre of the remnant. Most particles in the outskirts have angular momentum following the two tidal tails, one associated with the main progenitor, the other associated with the satellite. *Bottom-left*: same after removing both thin and thick disk: only the particles in the loops are kept. *Bottom-right*: distribution of angular momentum for all the particles associated to the tidal tail of the satellite, evidencing that these particles are lying in the  $\Phi=225$  degrees plane.

right panel shows two peaks which correspond to the two tidal tails formed after the second passage. The tidal tail associated to the main galaxy (see Fig. 2 at 4.2 or at 4.5 Gyr) is spiralling around the thick disk and its angular momentum peaks at  $\Phi=290$  degrees, which is indeed part of the thick disk (see top-left panel). This peak disappears in the bottom-left panel for which the thin and thick disks have been removed. The residual particles form another well identified peak at  $\Phi=225$  degrees. We have verified that they correspond to particles returning from the tidal tail of the satel-

lite: in the bottom-right panel, selected particles of the tidal tail of the satellite indeed show a very similar distribution with a peak at  $\Phi=225$  degrees, which is offset by 45 degrees from the disk angular momentum. Selection of these particles have been done in a rather crude way (see Fig. 2, panel at  $T=4.2$  Gyr): we simply "cut the tidal tail" at the time of its formation, up to the edge of the satellite. However this crude selection misses some particles, for example those which are stripped from the satellite at later phases (e.g. 3rd passage, see Fig. 2, panel at 4.5 Gyr). Comparing the counts of particles having an angular momentum around the  $\Phi=225$  degrees peak, we find that our selection recovers 90%, 70%, 40% and 15% within shells of 100-170kpc, 50-100kpc, 30-50kpc and 20-30kpc, respectively. As expected, particles at the very edge of the tidal tail are the most difficult to pre-select. Five Gyr after fusion those particles have returned to trajectories close to the galaxy centre.

Tracing the trajectories of selected particles in the tidal tail is very instructive: they correspond to an important component of the angular momentum which is at odd with the rotation of both the thick and thin disks (see Fig. 8).

Fig. 8 describes the temporal evolution of trajectories of tidal tail particles returning to the galaxy. When falling to the galaxy centre, the particles are looping around the galaxy with a pericenter at  $\sim 25$  kpc. These particles are describing several elliptical orbits -or loops- around the galaxy potential. We identified 4 of these loops although they might be more numerous. Fig. 8 shows that with increasing time, they show a precession around the galaxy as well as they are growing. This is because stars coming back from the tidal tail are returning from higher elevation at later epoch and are coming back with increasing energy. We also notice that loops are somewhat thick and as such, they could be better called tores.

The permanent rain of stars from the tidal tail ensures very long-term streams of stars within the galaxy outskirts well after the remnant phase. In-falling stars are trapped into elliptical orbits with the remnant galaxy right at the foci, which make the orbit stable. These orbits are those expected for extremely small satellites (single stars!), in absence of tidally induced forces. Loops are expected

to persists for several billion years<sup>4</sup> after fusion and, moreover, they are permanently fed by new particles coming from the tidal tail. These streams and loops are all within a common plane, 45 degrees from the PA of the rejuvenated disk as it is evidenced by Fig. 8 (panels h and i). This is our proposed model for the formation of the Giant Stream which indeed points towards the centre of the galaxy. Let us now examine how this model is compliant with several observations of the Giant Stream properties.

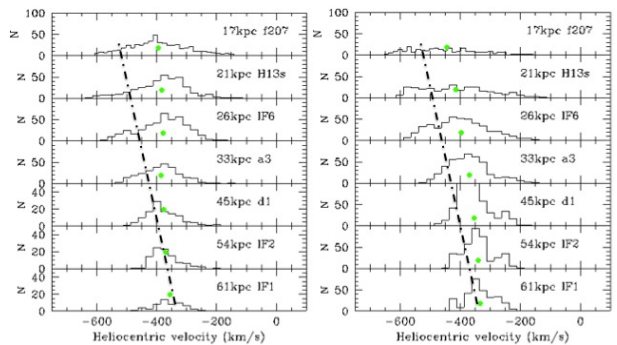


Fig. 9.— *Left:* Same model as in Fig 3. Distribution of heliocentric velocities in the Giant Stream region at distances indicated in each panels with references to fields from Gilbert et al. (2009). The dot-dashed line reproduces the black line of Figure 1 of Ibata et al. (2004) representing the high negative velocity edge. Green dots represents the mass weighted average for each panel. *Right:* Same for particles returning from the tidal tail. In this plot we have accounted for several snapshots in the simulation to artificially increase the number of stars in the central regions (see text).

The kinematics of stars follows the trend evidenced by Ibata et al. (2004) and Gilbert et al. (2009): stellar particles in the streams reach large negative values of their heliocentric velocities towards the centre (see panel i of Fig. 8). Fig. 9 shows the distribution of heliocentric velocities for stellar particles selected in the region of the Giant Stream within  $\Phi_{obs}$  from -90 to -140 degrees. Observations (see Fig. 1 of Ibata et al. (2004) and

<sup>4</sup>We have verified that the resulting dark matter density profile in the remnant is slightly oblate ( $e=0.2$ ) shortly after the fusion of the two galaxies and then stable: then it could not strongly affect the trajectories of returning star particles from the tidal tail.



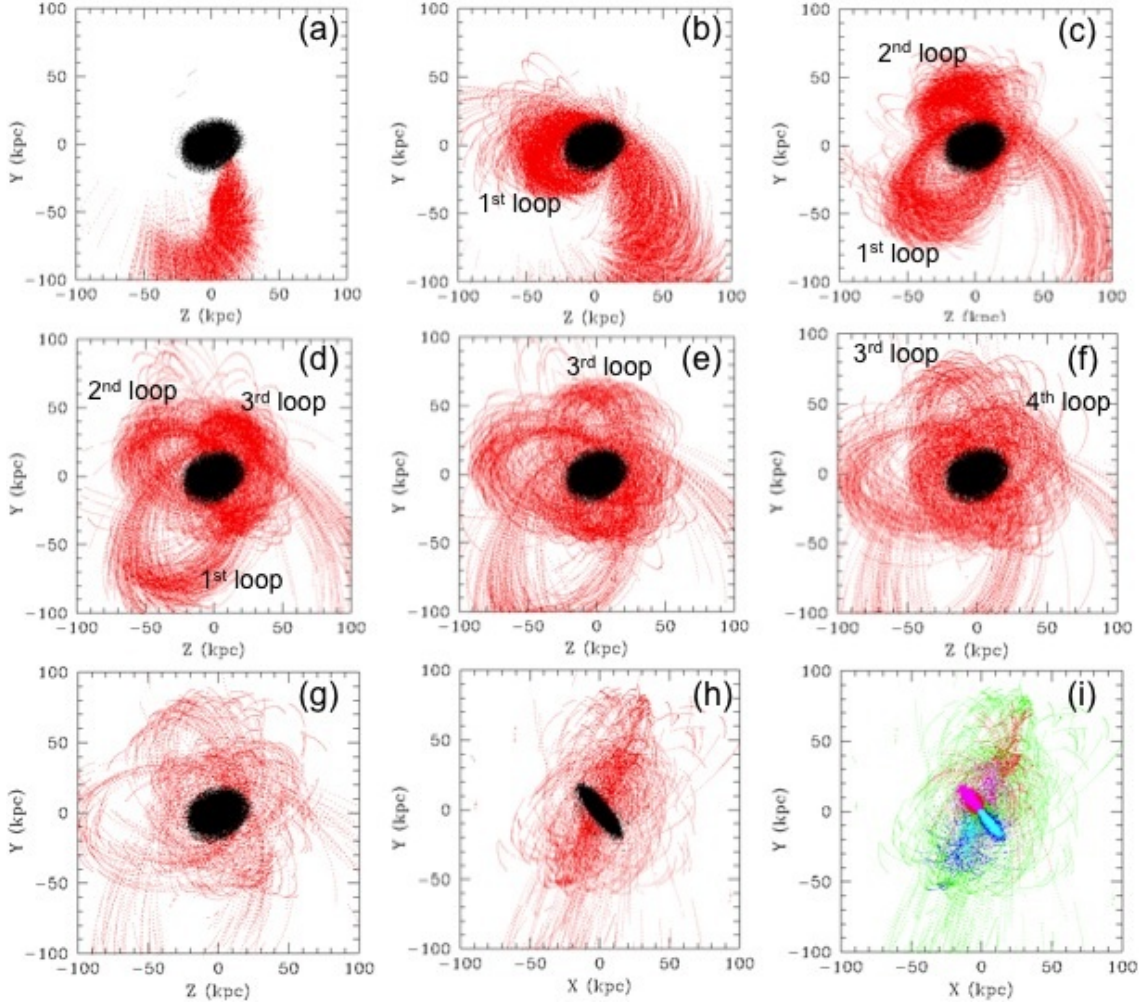


Fig. 8.— 2.8:1 merger with  $r_{\text{pericenter}}=30$  kpc. From panel (a) to (g): Snapshots in the (y, z) plane of trajectories for particles (red dots) which are part of the tidal tail of the satellite. Panel (a) shows the system just before fusion when particles are stripped from the satellite. Panels (b) to (f) show the particle motions for time intervals of 0-1Gyr, 1-2Gyr, 2-3Gyr, 3-4Gyr and 4-5Gyr after fusion, respectively. Panel (g) shows the distribution of particles 5.5 Gyr after fusion. For illustration, we have added in all panels the thin disk (black) as it is, 5.5Gyr after fusion. It shows the formation of the different loops which are drawn by particles when coming back from the tidal tail. Panel (h) and (i): Same as panel (g) but projected in the observer's frame in the (x, y) direction illustrating that the loops are inserted within a thick plane at 45 degree from the disk PA. Panel (h) shows the same particles than panel (i) for which the heliocentric velocities are coded following Chemin et al. (2009), i.e. cyan (<-500 km/s), blue (-500 to -400 km/s), green (-400 to -200km/s), red (-200 to -100 km/s) and magenta (> -100km/s). It illustrates a disk rotation very similar to the observed one as well as the velocity of the Giant Stream which is reaching larger negative velocities when it reaches the M31 centre.

Fig. 5 of Gilbert et al. (2009)) show a broadening of the velocity distribution towards the galaxy centre that is well reproduced by our simulations.

Besides this, our model reproduces also well the distribution of stellar ages observed by Brown et al. (2008), as we find 80%, 20% and 0% of stars

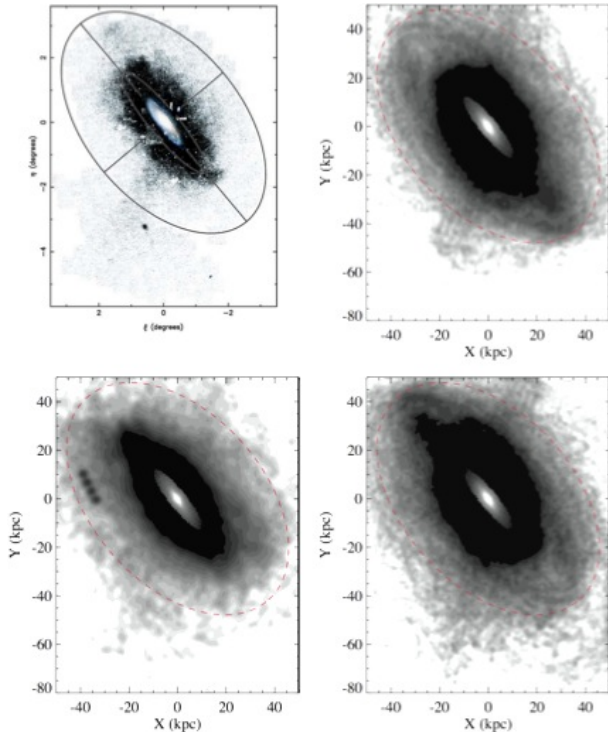


Fig. 10.— Comparison of observations (top-left from Ibata et al. 2005) with our modelling; on top-right, we adopted a mass ratio of 2.8:1 with  $r_{per}=30$  kpc observed after 10 Gyr, on bottom-left, a mass ratio of 3:1 with  $r_{per}=25$  kpc observed after 9 Gyr. The bottom-right panel shows the same than on top-right, except that we have inverted all axes. 4 to 10 snapshots have been used to optimise the contrast.

older than 8 Gyr, from 5 to 8 Gyr and younger than 5 Gyr, respectively. These fractions can be regulated by changing the feedback prescriptions (see section 4.2).

We have attempted to reproduce the photometric properties of the Giant Stream. The difficulty of such an attempt is due to the fact that the Giant Stream is very faint when compared to other substructures of M31, which is a problem also encountered by observers. Even with 500 000 particles, the number of stellar particles in the Giant Stream is below 1000 which obviously limits a detailed reproduction of the structure. Within an angle of  $\Phi_{obs}$  from  $-90$  to  $-140$  degrees and from 25 to 80 kpc, the total mass of the Giant Stream is  $4.8$  and  $4.4 \times 10^8 M_{\odot}$  in the two examples illustrated in Fig.

10. Using other variations of the model parameters we find a range from  $2$  to  $5 \times 10^8 M_{\odot}$ , which includes well the observational value of  $3 \times 10^8 M_{\odot}$  (see Mori & Rich 2008).

All our models (column 4 of Table 1) show streams of stars which belong to a plane that intersects the observational plane in a direction 45 degrees from the thin disk PA. We verify that to optimise the reproduction of the observed features in position and strength, we can use two different kinds of symmetry. First, we can rotate the whole system around an axis perpendicular to the thin disk, as this would not affect the galaxy decomposition in sub-substructures, nor the kinematics of thin and thick disks. Second, we find that gravity is not sensitive to a complete inversion of the initial (x, y, z) coordinate system. This has the advantage of being able to reproduce the Giant Stream with many variations of our model parameters. Also it has the inconvenience to provide a very large amount of space parameters to investigate. Fig. 10 illustrates some examples of this exercise for two models with 500K particles for which the Giant Stream mass is slightly larger than the observed one. Much larger number of particles are certainly required to reproduce at the same time all the morphological details of the thick disk, although we generally reproduce quite well the NE and W shelves.

## 5. Discussion and Conclusion

By construction, all models reproduce quite well the distribution of stellar ages in the various substructures, as they are described in Fig. 1. This is especially true for both the thick disk and the Giant Stream (see sections 4.2 and 4.4) for which our predicted compositions of stellar ages is from 10 to 20% of intermediate age stars (5-8 Gyr), the rest being essentially made of older stars. However, we experienced some difficulties to reproduce the distribution of the 21kpc and 35kpc "Halo" fields of Brown et al. (2008). We indeed find a fraction of intermediate age stars ranging from 5 to 15%, while it should be near or below 5% from Figure 1. It would be tempting to use this property for selecting the best model of M31. However, in our models intermediate age stars are related to low mass particles, three of them being produced by a single gas particle. It may lead to

an artificially scattering of those intermediate age star particles (see section 3), which could be only solved by simulations with a much larger number of particles than 500K.

All models as defined in Table 1, column 4 can reproduce with a quite good accuracy the bulge, thin and thick disk fractions, as well as the ring and the shape, the mass, and the kinematics of the Giant Stream. The examples shown in Fig. 10 are cases for which the Giant Stream stellar content is slightly larger than the observed one, for illustration purposes. We also notice that the shapes of the predicted thick disk and Giant Stream can significantly change -within a given set of orbital parameters (see Table 1)- either because they can be modified through a rotation around the disk axis or because they could fluctuate with the assumed time after the beginning of the simulation. It is beyond the scope of this paper to search for the best model that reproduce all the details of M31 substructures. This would need to launch several hundreds of simulations with several millions of particles. We have however learned from this analysis that:

- a thin disk as that of M31 can be reproduced with a combination of  $\sim 65\%$  of gas in the progenitors and a star formation history that prevents gas consumption before the fusion; low efficiency of star formation is thus predicted in primordial gaseous phases, while when the medium has been sufficiently enriched and mixed during fusion, the gas is more easily consumed; this transition has been essentially modulated through the assumed feedback history;
- the same star formation history reproduces as well a rotationally-supported thick disk with stellar composition similar to what is observed;
- and also fractions of bulge/thin disk and thick disk similar that what is observed within 10% accuracy.
- these polar orbits always reproduce the observed 10kpc ring, and in most cases, the gas map is very similar to the observed one (see Fig. 6), especially when the gas in the galaxy centre is allowed to form stars after the galaxy fusion;

- the predicted Giant Stream is made of stellar streams due to returning stars from a tidal tail formed prior fusion from stripped particles of the satellite; these stars are drawing streams along loops which are inserted into a thick plane that is 45 degrees inclined relatively to the disk PA (see Fig. 8); such streams are very long-lived because returning particles are trapped into such loops for periods larger than several Gyr, and also because the streams are permanently fed by new particles falling back from the tidal tail at all epochs.

The success of modeling M31 properties as resulting from a past major merger event is patent. Its predictive power is however limited by the complexity of the system as well as the very demanding number of particles required to reproduce in details all substructures of M31. An important limitation could be also the accuracy of the calculations, which imposes to track with an unprecedented accuracy positions and velocities of particles for almost a Hubble time. In fact, we cannot claim to have determined the best major merger model of M31, although they are likely within the limits discussed below.

We did not either try to investigate the whole parameter space to which the above results hold, although examination of Table 1 let us to suspect that it is likely large. However some specific links between parameters and observations may provide some empirical limits. The bulge fraction can be reached within a 10% accuracy for all models with mass ratio of  $3 \pm 0.5$ . In the frame of our model for M31, the halo is enriched by stars coming from the progenitors before the interaction, while thick disk and Giant Stream are further enriched by stars formed before first passage and fusion. This (see Figure 1 and section 2) is compliant with pericenter radii of  $25 \pm 5$  kpc. Further modelling and measurements of stellar ages in several fields in the outskirts of M31 would certainly help to provide more accurate values. This would also provide better accuracy to the important epochs of the interaction which would have begun  $8.75 \pm 0.75$  Gyr ago with a fusion time  $5.5 \pm 0.5$  Gyr ago. There is still work needed to constraint properly other orbital parameters such as inclinations of progenitors relatively to the angular momentum direc-



tion. We are far from having investigated the whole range of orbital properties which produces a strong tidal tail from stripped material from the satellite, and then a structure similar to the Giant Stream. Table 3 describes all the models presented in this paper, which are part of about 50 tested models. Fig. 6 evidences that models with difference of progenitors inclination near 180 degrees shows a maximum of resonance (thus very strong tidal tail) but also galactic disks which are probably too warped or distorted. We have mostly investigated models with the main galaxy inclination of 55 to 70 degrees, but there could be other solutions for different angles. All the models in Table 3, as well as models in the range described by Table 1 (4th column) are reproducing quite well the observations, including the Giant Stream. A much detailed analysis is necessary to determine the best model parameters, and this could be done by comparing in detail the constraints provided by the gaseous disk, the thick disk, and the Giant Stream shapes as well as by any other structures discovered in the M31 halo field.

During the writing of this paper, we have been aware of the discovery of many other structures in the halo of M31 (Mackey et al. 2010), especially after the successful deep imagery of the whole field surrounding M31 by the PANDA team (McConnachie et al. 2010). This magnificent image reveals the presence of loops which surrounds M31 which strikingly resemble to our model predictions (see Fig. 8). In particular the northern loop found by the PANDA team which extends up to 120 kpc from the galaxy centre provides particularly strong constraints on our model. Indeed the first loop in Fig. 8 can reproduce accurately the northern loop (called NW stream in the incomplete image of Mackey et al. 2010), and other loops are well matched with the Eastern arc and Stream C. Fig. 11 shows two examples of models that succeed to reproduce most of these features together with the Giant Stream and most other substructures (thin disk, bulge and thick disk) of M31. In fact we also verified that the Giant Stream kinematics is still reproduced. Fitting these additional structures allows us to fix the rotation angle around the thin disk axis as well as solving the initial conditions of the system because only the inversion of the initial (x, y, z) coordinate system is able to reproduce the ensemble of features in Fig. 11. The size of the

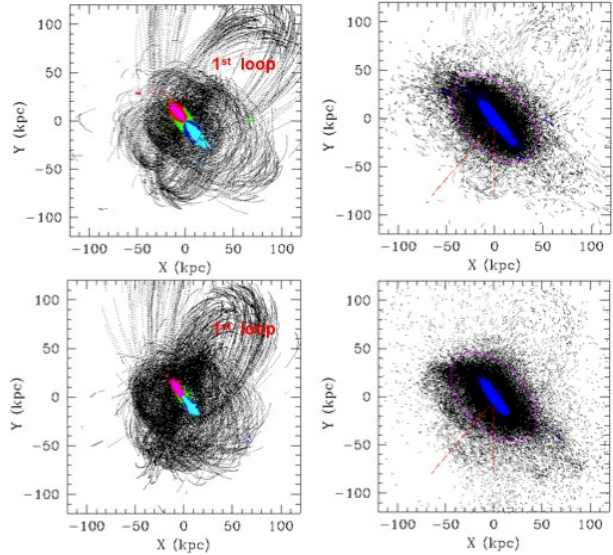


Fig. 11.— Two models for which most features have been reproduced including those from the new PANDA survey. *Top*: a model with 500K particles assuming a 3:1 merger,  $r_{per}=25$  kpc and inversion of the initial (x, y, z) coordinate system. On the left are shown the returning particles from the tidal tail as in Fig. 8, panels (h) and (i), with black dots and with the rotating disk inserted (same code than in Fig. 8). On the right all particles of the simulation are shown, including 4 snapshots around  $T=8.72$  Gyr. This model is with  $Gal1_{incy}=65$ ,  $Gal2_{incy}=-95$ ,  $Gal1_{incz}=85$ ,  $Gal2_{incz}=85$ , half the maximal feedback until 0.5Gyr after fusion, then low feedback. *Bottom*: a model with 1M particles assuming a 2.8:1 merger,  $r_{per}=30$  kpc and inversion of the initial (x, y, z) coordinate system. Here only 2 snapshots around  $T=9.05$  Gyr are shown in the left image. Here a constant high feedback history has been assumed and other parameters are  $Gal1_{incy}=65$ ,  $Gal2_{incy}=-89$ ,  $Gal1_{incz}=110$ ,  $Gal2_{incz}=110$ . The Giant Stream mass includes 2.5 to 2.8  $10^8 M_{\odot}$ .

loop also depends on the time elapsed after fusion and the beginning of the interaction is expected to be  $8.75 \pm 0.35$  Gyr within the range of parameters in Table 1.

As a whole, M31 and the complex structures in its halo can be reproduced by assuming a single major merger which may have begun 8.7 Gyr ago. The advantages of such a solution for M31 com-

Table 3: Summary of model parameters from Table 1 used throughout the paper (all within the range of parameters of Table 1, column 4). Angle, pericenter radii, number and mass of particles are given in degrees, kpc, 1000s of particles and ( $10^6 M_\odot$ ), respectively. Feedback adopted values are (1): high feedback; (2): 5 times medium feedback; (3) high feedback before fusion then low feedback and (4): 5 times medium feedback before fusion then low feedback. Model parameters for Fig. 4, 7, 8, 9 and 10 are the same than for Fig. 3; the other model used in Fig. 10 is the same than for Fig. 11a. The 6 last lines of the Table provides a check of the goodness of each model within  $\pm 20\%$  of the observed value: the decomposition of M31 in bulge, thin and thick disks (e.g.  $B/T=0.28\pm 0.05$ ), the disk scale length (e.g.  $5.8\pm 1.1$  kpc), the 10 kpc ring, the Giant Stream (e.g.  $3\pm 0.6 \cdot 10^8 M_\odot$ ), the stellar ages in the thick disk and in the Giant Stream (assuming fraction of  $> 8$  Gyr stars to be  $85\pm 8\%$ ) and gas fraction in the galaxy within 30 kpc ( $7\pm 2\%$ ).

parameter	Fig2	Fig3	Tab2a	Tab2b	Tab2c	Tab2d	Tab2e	Fig5 & Fig6b	Fig6a & Fig11a	Fig6c	Fig11b
mass ratio	3.0	2.8	3.5	3.0	2.8	2.5	2.5	3.0	3.0	3.0	2.8
Gal1 incy	70	65	60	65	65	65	65	65	65	65	65
Gal2 incy	-109	-89	-109	-89	-89	-89	-89	-95	-95	-105	-89
Gal1 incz	110	90	110	90	90	90	90	90	85	90	90
Gal2 incz	110	90	110	90	90	90	90	90	85	90	90
$r_{\text{pericenter}}$	24	30	24	24.8	24.8	24	24	24.8	24.8	26	30
Feedback	1	1	1	1	1	1	3	3	4	1	1
$N_{\text{particle}}$	300	300	154	300	159	300	159	540	540	300	960
$M_{DM}$	2.2	2.2	7.3	2.2	7.3	2.2	7.3	1.2	1.2	2.2	0.68
$M_{\text{oldstar}}$	1.1	1.1	1.8	1.1	1.8	1.1	1.8	0.6	0.6	1.1	0.34
$M_{\text{gas}}$	1.1	1.1	0.9	1.1	0.9	1.1	0.9	0.6	0.6	1.1	0.34
$M_{\text{newstar}}$	0.37	0.37	0.3	0.37	0.3	0.37	0.3	0.3	0.3	0.37	0.11
model goodness											
decomposition	OK	OK	OK	OK	OK	OK	NO	OK	OK	OK	OK
disk scale length	OK	OK	OK	OK	OK	OK	OK	OK	OK	OK	OK
10kpc ring	OK	OK	OK	OK	OK	OK	OK	OK	OK	OK	OK
Giant Stream	OK	OK	OK	OK	OK	OK	OK	OK	OK	OK	OK
stellar ages	OK	OK	OK	OK	OK	OK	OK	OK	OK	OK	OK
gas fraction	NO <sup>a</sup>	NO <sup>a</sup>	NO <sup>a</sup>	NO <sup>a</sup>	NO <sup>a</sup>	NO <sup>a</sup>	OK	OK	OK	NO <sup>a</sup>	NO <sup>a</sup>

<sup>a</sup>Models with a constant star formation with low efficiency (or high feedback) could not transform enough gas into stars after the fusion leading to more gas-rich disk than observed; assuming a varying star formation (more efficient after the fusion) suffices to correct the discrepancy.

pared to the hypothesis of numerous minor mergers are:

- it explains most of the complexity of M31 by a single event rather than numerous and minor merger events which have to be adapted in a somewhat ad-hoc way to each features discovered in the M31 halo, including the thick disk;
- it naturally explains stellar ages and metallicities of most substructures in the M31 halo as well as why they show so much similarities;
- it overcomes the increasing difficulty of identifying the residuals of satellites assumed to be responsible of the different features in the M31 halo;
- it is consistent with the kinematics of the

M31 globular system (e.g., Bekki 2010).

Re-formation of disks is expected after gas-rich major mergers (Barnes, J.E. 2002; Springel 2005). It is more than just a curiosity since the disk rebuilding scenario has been proposed as a channel for the general formation of spirals (Hammer et al. 2005), including specifically the case of M31 (Hammer et al. 2007). Gas-richness of progenitors is certainly high, as it has been estimated for many high- $z$  galaxies. The requirement of a star formation with a low efficiency before the fusion can be reached through any mechanism that prevents star formation in relatively primordial medium. It could be either caused by higher feedback efficiency in primordial medium as assumed in section 4.2, or because the gas in the progenitors is less concentrated than in present-day spirals as it is in present-day low surface brightness galaxies or because cooling is less efficient in rel-

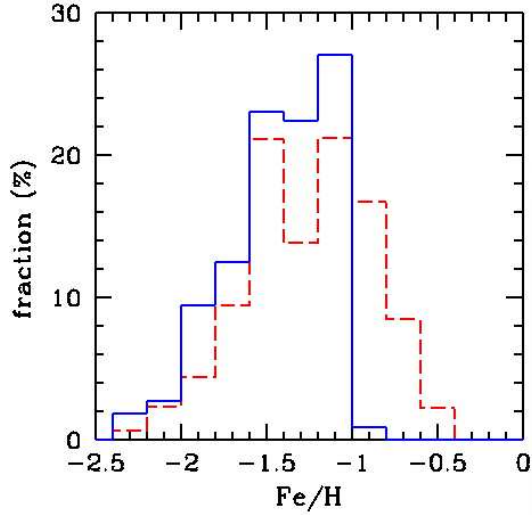


Fig. 12.— Fe/H distribution of progenitor stars in the Giant Stream (red dashed line) and in the northern loop (blue solid line), for the same model than in Fig. 11a. The absence of metal rich stars (e.g.  $-0.4 < \text{Fe}/\text{H} < 0$ ) is due to the fact that particles returning from the tidal tail are coming from the outskirts of the progenitors. The absence of stars richer than  $\text{Fe}/\text{H} = -0.7$  could explain why the northern loop is not detected with such a metallicity selection, while it becomes prominent for metal poor stars ( $\text{Fe}/\text{H} < -1.4$ ).

atively pristine medium or a combination of all these factors. More generally the expected increase of the gas metal abundance (expected to be slow before the fusion but very efficient during the fusion) may help to increase the molecular gas fraction, the optical depth of the gas and the radiation pressure effects, all contributing to a change in the star formation history during the interaction (TJ Cox, private communication). The above is quite well illustrated *a contrario* by Bournaud et al. (2010) who assumed that progenitors of high- $z$  major mergers are very strong star forming, turbulent, gas-rich disks: they naturally find that remnants cannot be disk dominated within such conditions.

There is still a considerable need to improve the modelling of M31, by using a much larger number of particles as well as by providing more kinematical and stellar age constraints in the numerous fields of view surrounding M31. We also

need to reproduce with more accuracy the shape of the Giant Stream and of the thick disk contours. Metal abundance enrichment can be also implemented to fit more accurately the observations. For example the striking differences between features at different metallicity in the halo found by the PANDA team cannot be retrieved by our modelling in absence of such an implementation<sup>5</sup>. We have attempted to verify whether such a trend is predicted by our model. At first order, one may “paint” each star in the progenitors assuming a reasonable metallicity gradient. We adopt the approach by Rocha et al. (2008) assuming that metallicity gradient follows the dust gradient, with a scalelength 1.4 times larger than that of the stars. The range of metal abundance ( $\text{Fe}/\text{H}$ ) is adopted from 0 to -2.5. The stellar metal abundance of the satellite is likely significantly smaller than that of the main progenitor, because their stellar mass ratio (for our 3:1 models, see Table 1) is 5. Little is known about the shape of the metal-stellar mass relationship at  $z \sim 1.5$ , although a serious attempt has been done at  $z \sim 0.7$  by Rodrigues et al. (2008). Assuming this holds up to  $z=1.5$ , stars in the main progenitor are on average 0.4 dex more metal rich than those from the satellite, a value smaller than the large scatter of the Rodrigues et al. (2008) relationship. Figure 12 shows the metallicity distribution of “painted” stars in both the Giant Stream (defined as in section 4.4, from 25 to 80 kpc and  $\Phi_{\text{obs}}$  from -90 to -140 degrees) and in the northern loop (defined from 55 to 130 kpc and  $\Phi_{\text{obs}}$  from 0 to 90 degrees) discovered by the PANDA team. Because most of the stars in the northern loop are coming from the satellite, this could explain why this feature is not detected in the metal-rich map of the PANDA team (see Fig. 12). Such a prediction may stand unless intermediate age stars (those formed before the fusion) strongly affect the metal abundance of both the Giant Stream and the northern loop. On the other hand the same model correctly predicts the (observed) small fraction of such stars in the Giant Stream.

<sup>5</sup>This may also help to better reproduce the 35kpc halo field of Brown et al. (2007) which is in-between the Eastern arc and the stream C (Mackey et al. 2010): this points out also the need for resolving stellar streams and then for a better accuracy in following positions and velocities of particles; similar need is for identifying carefully the particles in loops such as proposed for the Northern loop.

Another important improvement of this modelling would be to consider the possible interaction of M33 which has been proposed to be responsible for several features in the SE of the M31 halo by McConnachie et al. (2009). Although the dark matter density profile does not significantly affect our results (results shown in Fig. 2, 3, 4, 5, 7, 8, 9 and 11 are similar when using an Hernquist profile instead of a core profile), we also need to verify whether these are affected by adopting different baryonic mass fractions, especially for lower values than our adopted 20%. Indeed, considerable change of the dark matter fraction may prevent stars to be stripped by the collision and then the distribution of baryonic matter in the outskirts may be significantly affected.

However we believe the result of such a model is very encouraging because it fulfill the Occam's razor principle: a single event may explain most -if not all- the properties of M31 and of its outskirts. It also proposes a mechanism for the Giant Stream which is simply fed by stars which are captured into loops orbiting around M31 for elapsed times which may reach a Hubble time. If M31 is actually the result of an ancient major merger, there will be a considerable need to revise our knowledge about our immediate environment and in cosmology<sup>6</sup>, because:

- merging of gas-rich distant galaxies can easily produce large thin disks by assuming a less efficient star formation before the fusion; this simple scheme supports the rebuilding disk scenario for many giant spiral galaxies at least for those sharing similar properties (enriched halo stars) than M31;
- most models show the formation of tidal dwarves, including from tidal tails formed after the first passage, and some of them could be part of the satellite system of M31; their properties, after comparison with observations, may be used in the future as a constraint to the orbital parameters in further

modelling;

- up to 15% of the material is ejected after the fusion and this may populate the whole Local Group including in the direction of the Milky Way; this leads Yang & Hammer (2010) to investigate to which conditions the LMC might be related to some material coming from M31.

*Note added into proofs:* The specific frequency of globular clusters in M31 appears to be three or four times greater than it is in the Galaxy van den Bergh (2010), i.e., it is expected if a major merger occurred in the first galaxy. The fact that the globulars in M31 and in the Galaxy have almost exactly the same half light radii supports the notion that M31 formed by merger of two Galaxy-sized ancestors (Sidney van den Bergh, private communication) .

This work has been supported by the China-France International Associated Laboratory "Origins" and by National Basic Research Program of China (973 Program), No. 2010CB833000. Part of the simulations have been carried out at the High Performance Computing Center at National Astronomical Observatories, Chinese Academy of Sciences as well as at the Computing Center at Paris Observatory. We warmly thank Tom Brown, TJ Cox and Sidney van den Bergh for their very useful comments during the submission process of this paper. Suggestions and comments from an unknown referee have been very useful to improve the current version of the article.

## REFERENCES

- Abadi, M. G., Navarro, J. F., Steinmetz, M., & Eke, V. R. 2003, *ApJ*, 591, 499
- Baade, W. & Arp, H., 1964, *ApJ*139, 1027
- Barnes, J.E. 2002, *MNRAS*, 333, 481
- Bekki, K. 2010, *MNRAS*, 401, L58
- Beasley, M. A., Brodie, J. P., Strader, J., Forbes, D. A., Proctor, R. N., Barmby, P., & Huchra, J. P. 2004, *AJ*, 128, 1623
- Block, D. L., et al. 2006, *Nature*, 443, 832
- Bournaud, F., et al. 2010, *arXiv:1006.4782*

<sup>6</sup>the history of the galaxy formation theory has been strongly influenced by our knowledge of the Milky Way and the theory of spiral galaxy formation a la Eggen et al. (1962) is still lively; the fact that the second most nearby galaxy, M31, could be plausibly a major merger may remind us that the theory of galaxy formation could require significant adjustments.

- Braun, R., Thilker, D. A., Walterbos, R. A. M., & Corbelli, E. 2009, *ApJ*, 695, 937
- Bromm, V., Yoshida, N., Hernquist, L., McKee, C. 2009, *Nature*,
- Brown, T. M., Smith, E., Ferguson, H. C., Rich, R. M., Guhathakurta, P., Renzini, A., Sweigart, A. V., & Kimble, R. A. 2006, *ApJ*, 652, 323
- Brown, T. M., et al. 2007, *ApJ*, 658, L95
- Brown, T., et al. 2008, *ApJ*, 685, 121
- Byrd, G. G. 1978, *ApJ*, 226, 70
- Byrd, G. G. 1983, *ApJ*, 264, 464
- Carignan, C., Chemin, L., Hutchmeier, W. K. & Lockman, F. J. 2006, *ApJ*, 641, L109
- Chemin, L., Carignan, C., & Foster, T. 2009, *ApJ*, 705, 1395
- Cox, T. J., Jonsson, P., Primack, J. R., & Somerville, R. S. 2006, *MNRAS*, 1255
- Cox, T. J., Jonsson, P., Somerville, R. S., Primack, J. R., & Dekel, A. 2008, *MNRAS*, 384, 386
- Daddi, E., et al. 2010, *ApJ*, 713, 686
- Delgado-Serrano, R.; Hammer, F.; Yang, Y. B.; Puech, M.; Flores, H.; Rodrigues, M. 2010, *A&A*, 509, 78
- Eggen, O. J., Lynden-Bell, D., & Sandage, A. R. 1962, *ApJ*, 136, 748
- Fardal, M. A., Babul, A., Guhathakurta, P., Gilbert, K. M., & Dodge, C. 2008, *ApJ*, 682, L33
- Fardal, M., Guhathakurta, P., Gilbert, K., Babul, A., Dodge, C., Weinberg, M. D., & Lu, Y. 2009, *Astronomical Society of the Pacific Conference Series*, 419, 118
- Ferguson, A. M. N., Johnson, R. A., Faria, D. C., Irwin, M. J., Ibata, R. A., Johnston, K. V., Lewis, G. F., & Tanvir, N. R. 2005, *ApJ*, 622, L109
- Font, A. S., Johnston, K. V., Guhathakurta, P., Majewski, S. R., & Rich, R. M. 2006, *AJ*, 131, 1436
- Font, A. S., Johnston, K. V., Ferguson, A. M. N., Bullock, J. S., Robertson, B. E., Tumlinson, J., & Guhathakurta, P. 2008, *ApJ*, 673, 215
- Gilbert, K. M., et al. 2009, *ApJ*, 705, 1275
- Gordon, K. D., et al. 2006, *ApJ*, 638, L87
- Governato, F., Willman, B., Mayer, L., Brooks, A., Stinson, G., Valenzuela, O., Wadsley, J., & Quinn, T. 2007, *MNRAS*, 374, 1479
- Hammer, F., Flores, H., Elbaz, D., Zheng, X. Z., Liang, Y. C., & Cesarsky, C. 2005, *A&A*, 430, 115
- Hammer, F., Puech, M., Chemin, L., Flores, H., & Lehnert, M. 2007, *ApJ*, 662, 322
- Hammer, F., Flores, H., Puech, M., Yang, Y. B., Athanassoula, E., Rodrigues, M., & Delgado, R. 2009, *A&A*, 507, 1313
- Hopkins, P. F., Hernquist, L., Cox, T. J., Younger, J. D., & Besla, G. 2008, *ApJ*, 688, 757
- Hopkins, P. F., Cox, T. J., Younger, J. D., & Hernquist, L. 2009, *ApJ*, 691, 1168
- Hopkins, P. F., & Quataert, E. 2010, *MNRAS*, 405, 41
- Hopkins, P. F., Cox, T. J., Younger, J. D., & Hernquist, L. 2009, *MNRAS*, 397, 802
- Ibata, R., Irwin, M., Lewis, G., Ferguson, A. M. N., & Tanvir, N. 2001, *Nature*, 412, 49
- Ibata, R., Chapman, S., Ferguson, A. M. N., Irwin, M., Lewis, G., & McConnachie, A. 2004, *MNRAS*, 351, 117
- Ibata, R., Chapman, S., Ferguson, A. M. N., Lewis, G., Irwin, M., & Tanvir, N. 2005, *ApJ*, 634, 287
- Ibata, R., Martin, N. F., Irwin, M., Chapman, S., Ferguson, A. M. N., Lewis, G. F., & McConnachie, A. W. 2007, *ApJ*, 671, 1591
- McConnachie, A. W., et al. 2009, *Nature*, 461, 66
- McConnachie, A. W. et al. in "Stellar populations in the cosmological context", held at STScI, 2010 May Symposium
- Mackey, A. D., et al. 2010, *ApJ Letters*, 717, L11

- Mori & Rich, 2008, *ApJLetters* 674, L77
- Neichel, B., et al. 2008, *A&A*, 484, 159
- Nieten, C., Neininger, N., Guélin, M., Ungerechts, H., Lucas, R., Berkhuijsen, E. M., Beck, R., & Wielebinski, R. 2006, *A&A*, 453, 459
- Peñarrubia, J., McConnachie, A., & Babul, A. 2006, *ApJ*, 650, L33
- Puech, M., Flores, H., Hammer, F., Yang, Y. B. et al. 2008, *A&A*, 484, 173
- Puech, M., Hammer, F., Flores, H., Delgado-Serrano, R., Rodrigues, M., & Yang, Y. 2010, *A&A*, 510, A68
- Rich, R. M. 2004, in "Origin and Evolution of the Elements, from the Carnegie Observatories Centennial Symposia", published by Cambridge University Press, as part of the Carnegie Observatories Astrophysics Series. Edited by A. McWilliam and M. Rauch, 2004, p. 258
- Rocha, M., Jonsson, P., Primack, J. R., Cox, T. J. 2008, *MNRAS*, 383, 1281
- Roberts, M.S., 1966 *ApJ*, 144, 639
- Rodrigues, M., Hammer, F., Flores, H., et al. 2008, *A&A*, 492, 371
- Sato & Sawa 1986, *PASJ*, 38, 63
- Springel, V. 2005, *MNRAS*, 364, 1105
- Springel, V., & Hernquist, L. 2005, *ApJ*, 622, L9
- Tanaka, M., Chiba, M., Komiyama, Y., Guhathakurta, P., Kalirai, J. S., & Iye, M. 2010, *ApJ*, 708, 1168
- Thilker, D. A., Braun, R., Walterbos, R. A. M., Corbelli, E., Lockman, F. J., Murphy, E., & Maddalena, R. 2004, *ApJ*, 601, L39
- van den Bergh, S., 2005, in *The Local Group as an Astrophysical Laboratory*, ed. M. Livio & T. M. Brown (Cambridge: Cambridge Univ. Press), P.1-15 (astro-ph /0305042)
- van den Bergh, S., 2010 *AJ*, 140, 1043
- van der Kruit, P., 2007 *A&A* 466, 883
- Wang, J. L., 2010, in preparation
- Westmeier, T., Braun, R., & Thilker, D. 2005, *A&A*, 436, 101
- Wetzstein, M., Naab, T., & Burkert, A. 2007, *MNRAS*, 375, 805
- Yang, Y., Flores, H., Hammer, F., et al. 2008, *A&A*, 477, 789
- Yang, Y., & Hammer, F. , 2010, submitted to *ApJ*